韓國鑛物學會誌 第 5 卷 第 2 號(1992)
J. Miner. Soc. Korea, 5, 79－92(1992)

Mineralogy of Clay Minerals from the Sarisan Mine, Korea

麗州 싸리산 鑛山에서 産出하는 粘土鑛物에 對한 鑛物學的 硏究

Geon-Young Kim (김건영) · Soo Jin Kim (김수전)

Department of Geological Sciences, Seoul National University, Seoul 151-742, Korea
(서울대학교 지질과학과)

ABSTRACT: The Sarisan clay deposits of hydrothermal origin are found in the intensely weathered two-mica granite in Yeoju area. The major clay minerals of the Sarisan mine are illite and montmorillonite with minor disordered kaolinite, vermiculite, and some interstratified mineral. Clay minerals were studied using various methods including X-ray diffraction, infrared absorption spectroscopy, electron microscopy, and thermal and chemical analyses.

Illites occur as discrete illite or highly illitic interstratified mineral. They are of 1M and $2M_1$ polytypes and characterized by a low lattice charge (0.768-0.926 per unit formula), low K^+ content (0.741-0.902 per unit formula), and high Si/Al ratio (1.154-1.293) as compared with muscovite. Montmorillonites are highly negative charged and occasionally random-interstratified as I/S with 80-98% smectite.

Hydrothermal alteration is more important than later weathering alteration for the formation of illite and montmorillonite clay minerals. The hydrothermal alteration took place through two stages; the formation of illite in the early stage and the formation of montmorillonite in the late stage. Disordered kaolinite and vermiculite are the weathering products of plagioclase and biotite, respectively.

요약 : 열수기원의 싸리산점토광상이 여주지역의 매우 심하게 풍화된 복운모화강암내에서 발견된다. 싸리산광산에서 산출하는 점토광석은 주로 일라이트와 몬모릴로나이트로 이루어져 있으며 이외에 구조적으로 무질서한 카올리나이트, 버미큘라이트, 드물게 혼합층상광물 등이 소량으로 산출된다. 이들 점토광석에 대한 연구를 위하여 X선회절분석, 적외선흡수분광분석, 전자현미경관찰, 열분석 및 화학분석 등을 실시하였다.

일라이트는 순수한 일라이트, 혹은 대부분 일라이트층으로 이루어진 혼합층상광물로서 산출한다. 1M과 $2M_1$의 두가지 다형이 있으며 이들은 백운모에 비하여 낮은 격자내 전하(단위 화학식당 0.768-0.926), 낮은 K^+함량 (단위 화학식당 0.741-0.902), 높은 Si/Al 비 (1.154-1.293)로 특징지워진다. 몬모릴로나이트는 높은 전하를 가지며, 경우에 따라서는 80-98% 스멕타이트층으로 이루어진, 불규칙한 혼합층상광물로 산출하기도 한다.

일라이트와 몬모릴로나이트와 같은 점토광물은 주로 열수변질작용에 의하여 생성되었을 것이다. 이 열수변질작용은 두 시기에 걸쳐서 일어난 것으로 보인다. 초기에는 일라이트를 생성시켰고, 후기에는 몬모릴로나이트를 생성시켰다. 구조적으로 무질서한 카올리나이트와 버미큘라이트는 각각 사장석과 흑운모의 풍화산물이다.

INTRODUCTION

The clays in the Sarisan clay deposits consist chiefly of montmorillonite and illite. They are used for manufacturing white wares. The Sarisan mine produces about 300-500 tons per month. The mine is located in Buknae-Myeon and Daesin-Myeon, Yeoju-Gun, Kyeongki-Do, Korea (Lat. 37° 18'-37° 21', Long. 127° 37'-127° 41').

Geological map of Yeoju quadrangle on the scale of 1:50,000 including the southern part of the study area was published by Yeo and Lee (1975).

The Sarisan clay deposits were investigated by the Korea Mining Promotion Corporation (1987). But any mine ralogical study has not yet been carried out in details. This study is the first mineralogical investigation of the Sarisan clay deposits.

The purpose of the present study is to identify the clay minerals of the clay deposits and investigate their mineralogical and genetic characteristics by various experimental methods.

In this study, illite refers to the nonexpanding dioctahedral, aluminous, potassium mica-like clay minerals that have a 10 Å basal repeat unit (Srodon and Eberl, 1984), show no evidence of interstratification but nevertheless contain less K^+ than true mica (Gaudette et al., 1966), and illitic material is used as a group name implying the possible presence of some expandable layers.

The name smectite refers to the expandable clay minerals with layer charge between 0.2 and 0.6 per formula unit, and montmorillonite is used for dioctahedral smectite (Bailey, 1980).

GEOLOGICAL BACKGROUND

Geology of Yeoju Area

Geology of the study area is mainly composed of granitic rocks of Jurassic age (Figure. 1). They are composed of two-mica granite, biotite granite, and quartz monzonite. The mineral compositions of granitic rocks determined by modal analysis are given in Figure. 2.

Two-mica granite is distributed in the western and southern parts of this area. It is coarse-grained granular in texture and brownish gray or milky gray in color (Fig. 3A). Almost equal amo-

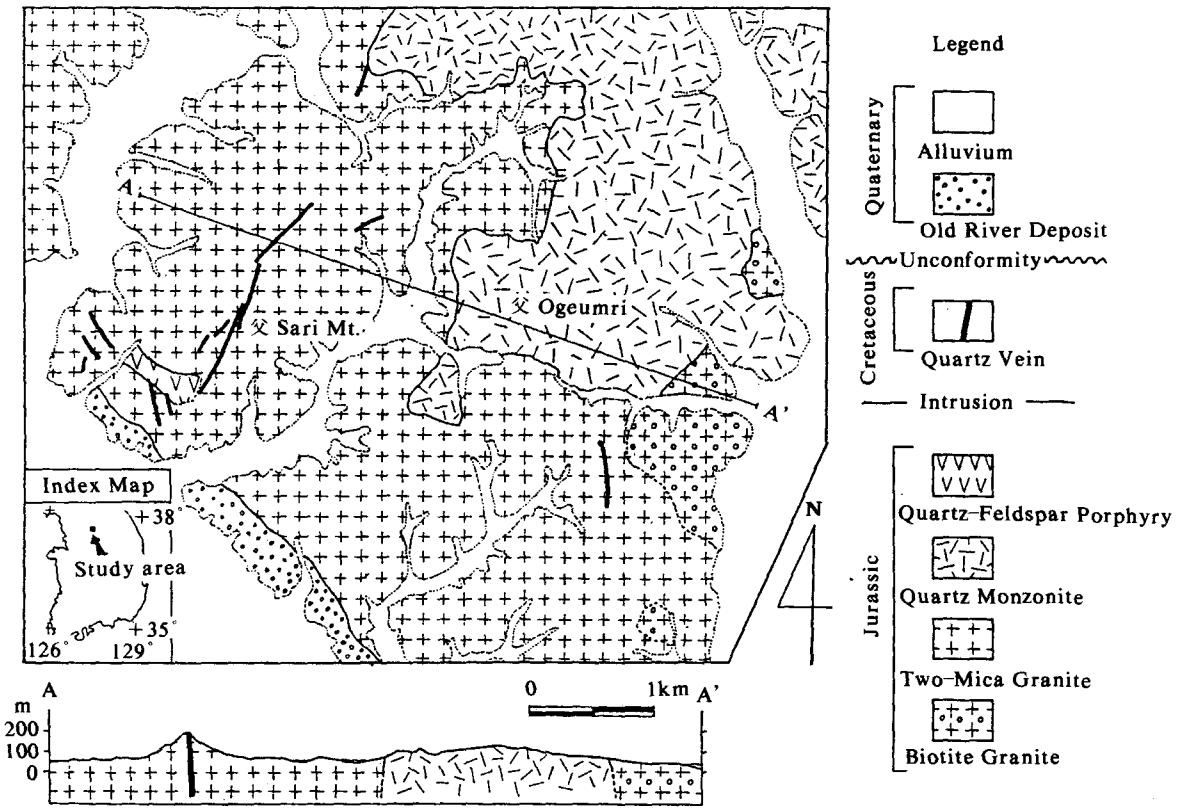

Fig. 1. Geological map of the Yeoju area.

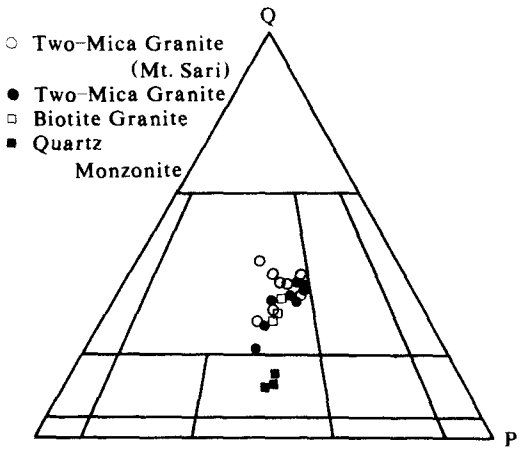

Fig. 2. Modal compositions of the Yeoju granite and quartz monzonite plotted on Streckeisen's Q A P diagram.

unts of biotite and muscovite are contained in the two-mica granite. Biotite granite is characterized by its granular texture and dark brownish gray color. Biotite granite grades gradation to two-mica granite. Irregular joint patterns are common in these granites.

Quartz monzonite is distributed near Ogeum-ri in the northeastern part of the study area (Fig. 1). The rock is fine-grained and pale greenish gray or milky greenish gray in color.

Quartz-feldspar porphyry intrudes two-mica granite in the southwestern part of Mt. Sari and shows porphyritic texture with the phenocryst of quartz or feldspar and the groundmass of fine-grained quartz or feldspar.

Quartz vein intrudes the granitic rocks in Sarisan mine along the ridge of Mt. Sari trending N30°E. It varies from several 10s cm to 10m in width (Fig. 3C).

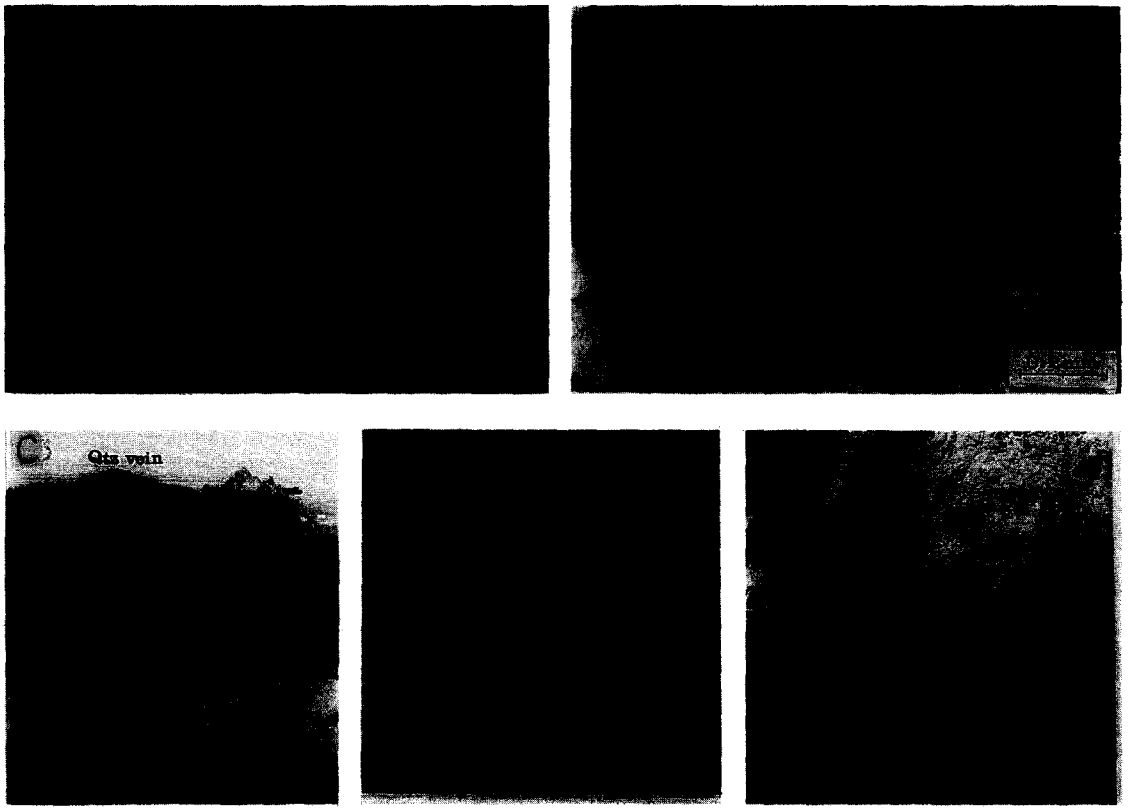

Fig. 3. (A) Handspecimen of two-mica granite. (B) Plagioclase in slightly altered two-mica granite. (C) View of quartz vein in Sari Mt. (D) Highly altered two-mica granite and (E) Clay vein.

Because of intense weathering, the topography of the study area is characterized by low hills and deep weathered zone.

Clay Deposits

The main constituent clay minerals of the Sarisan clay deposits are illite and smectite. It seems that they are primarily hydrothermal alteration products of two-mica granite, which have been subjected to later intense weathering process. They have various colors; yellow, greenish gray, green, brown, pink, and white. Clay deposits occur in two types: highly weathered two-mica granite and vein;

Clay formed by deep weathering of two-mica granite preserves the original texture of parent rocks (Fig. 3D). It is widely distributed in the Sarisan mine. Main constituent clay mineral is illite, and it is mined mainly in the open pits. Although illitic clay in the weathered granite is usually lower in grade than that in vein type, the former is much more abundant than the later.

Vein clay occurs discontinuously along the Sarisan quartz vein (Fig. 3E). It contains quartz grains of various sizes. In places, the altered two-mica granite fragments are included in the vein just like xenolith. Smectite is usually admixed with varing amount of illite. Therefore, it is hard to collect pure smectite sample. Vein clay is mined usually in underground.

EXPERIMENTAL METHODS

Geological investigation was carried out to prepare the geological map of the Yeoju area and to know the occurrence of clay minerals. Rock and clay samples were collected systematically considering their color, texture, and the degree of weathering.

Several undisturbed clay-rich samples were impregnated with araldite AY-103 low viscosity resin in a vacuum to prepare the polished thin sections for optical examination and electron microprobe analysis.

Separation of pure clay minerals was successful by centrifuging or hand-picking under stereomicroscope. Smectite minerals were easily separated by centrifuging because of their extremely small size. In order to avoid that dramatic improvements of diminution on the XRD peak intensity and to represent the natural clay system (Brewster, 1980), samples were not chemically treated. Some prepared samples were saturated with various cations following the methods by Jackson (1969).

The morphology and textures of minerals were studied using polarizing microscope, JEOL JXA-733 scanning electron microscope (SEM), and JEOL JEM 200CX transmission electron microscope (TEM).

The mineral identification and characterization as well as the relative mineral contents of both the bulk and prepared samples were determined using JEOL Model JDX-5P diffractometer and Rigaku, Model RAD-3C with Ni-filtered CuKα radiation, Slits were selected so that the X-ray beam divergence was less than the sample length. Scanning speed was adjusted to the purpose. For accurate measurement of d-spacing, powdered quartz and tetradecanol were used as standard (Brindley and Brown, 1980).

Infrared absorption spectra were recorded by Perkin-Elmer 283B Spectrophotometer, and DTA and TG curves were simultaneously obtained with Rigaku instrument.

pH values of smectites were measured with DMS Model DP-135 digital pH meter in water suspension following the methods of Jackson (1969).

Chemical analyses of minerals were carried out using JEOL JXA-733 electron microprobe.

Homogenization temperatures of fluid inclusions from Sarisan quartz vein were measured by USGS type Gas Flow Heating and Freezing System.

CLAY MINERALOGY

Clay minerals identified from Sarisan clay deposits are montmorillonite, illite, disor dered kaolinite, vermiculite, and some interstratified minerals.

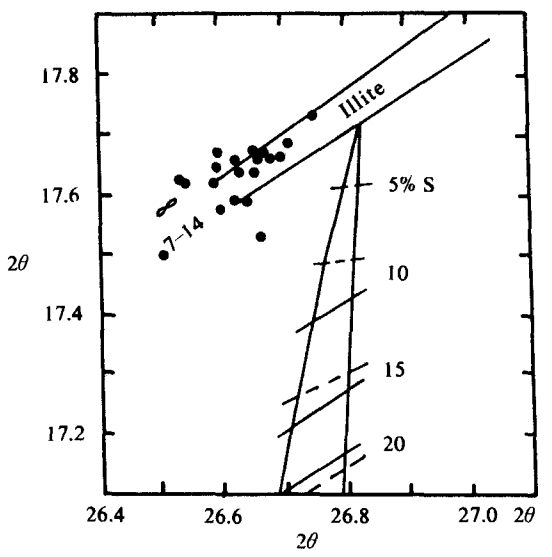

Fig. 4. Plotting of 2θ angles of (002) and (003) reflections of ethylene glycolated specimens on the Srodon's(1984) diagram.

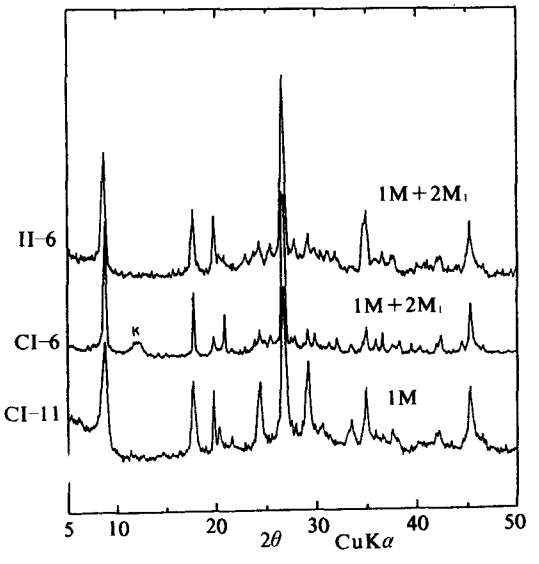

Fig. 5. X-ray diffraction patterns of two polytypes of illite.

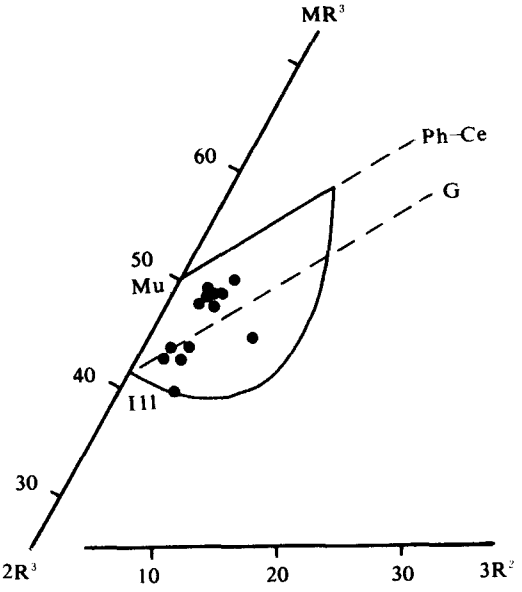

Fig. 6. Plotting of chemical compositions of illite in the Sarisan mine on the Velde's(1985) MR^3-$2R^3$-$3R^2$ coordinates. $MR^3=Na+K+2Ca$, $3R^2=(Mg+Fe^{2+})/3$, $2R^3=(Al+Fe^{3+}-MR^3)/2$. Mu:muscovite, Ph-Ce:phengite-celadonite compositions, G:glauconite-type composition, Ill:illite.

Illite

Identification of illite was carried out following Srodon's (1984) and Srodon and Eberl's (1984) procedures. These techniques require analysis of both air-dried and ethylene glycol solvated preparations.

Table 1 presents the measured data for the most of the samples used in this study. The peak positions of illitic materials are plotted in the illite or illite-dominated mixture field in Figure. 4, and their intensity ratios indicate that they have some expanding components except for the TI-4, CI-6, and CI-11 samples. The last two columns of Table 1 are the results of determination of the percentage and type of interstratification. Most of illitic materials from Sarisan mine are the mixture of discrete illite and ISII ordered I/S (<15% S). This fact indicates that the illitic materials are nearly pure illite. Two polytypes of illite, that is,

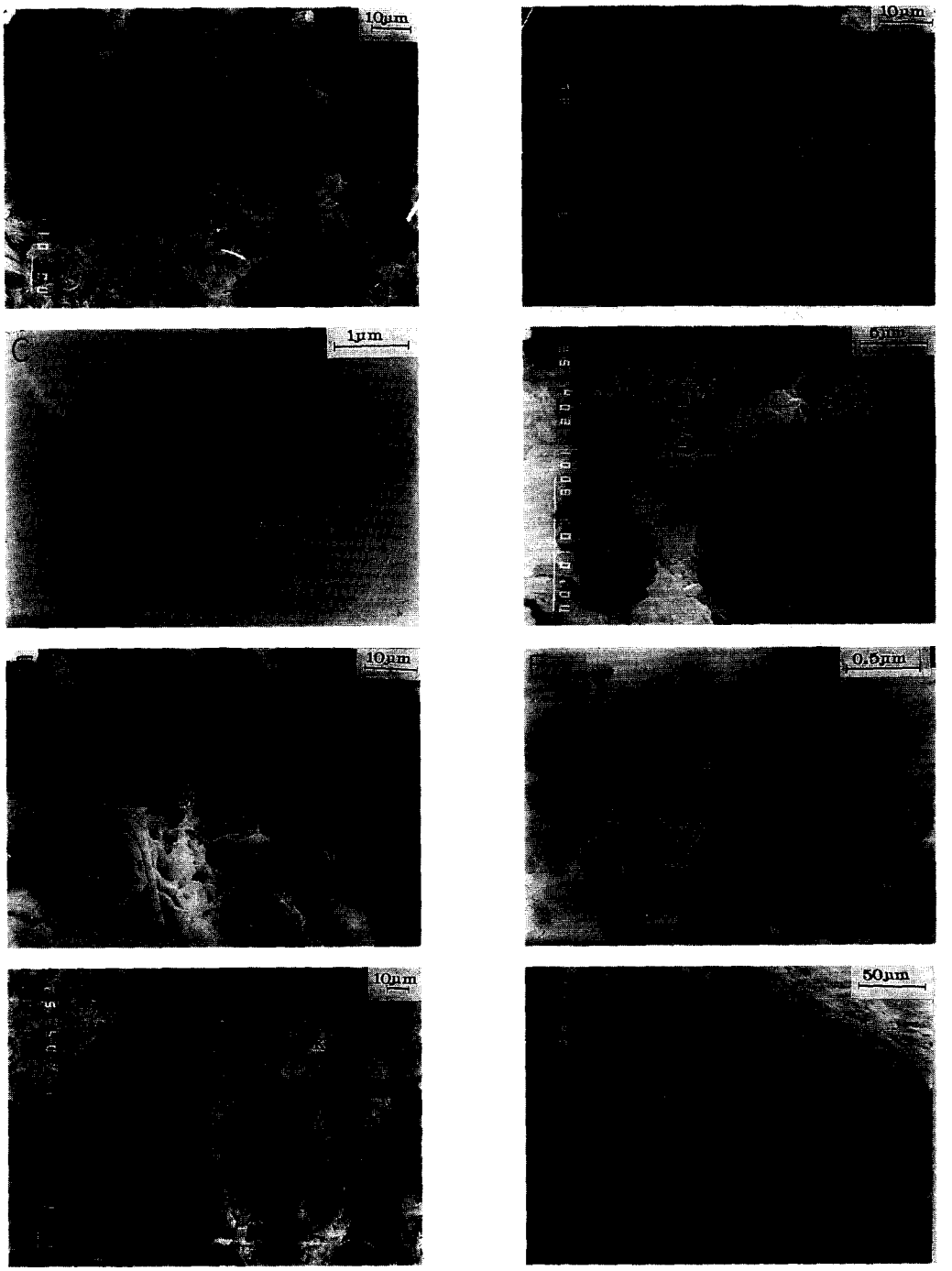

Fig. 7. SEM (A, B, D, E, G, H) and TEM (C, F) photographs. (A), (B) Poorly defined illite flakes. (C) Hexagonal illite. (D), (E) Curled montmorillonite along muscovite edges. (F) Irregular mossy montmorillonite(M) and discrete illite(I). (G) Kaolinite showing book structure (arrows) and etch pits on plagioclase. (H) Central biotite transformed into the lateral vermiculite. Mu:muscovite, Q:quartz, Ksp:K-feldspar, Pl:plagioclase, Bio:biotite, Verm:vermiculite.

Table 1. Measured data for identification of illitic materials from the Sarisan mine.

Sample No.	[a]$\Delta_{002-001}$ (2θ)	[b]BB1 (2θ)	[c]BB2 (2θ)	[d]Ir	%S	Type
AI-2	8.85	–	1.72	1.73	5	I+ISII
AI-8	8.86	–	0.96	1.51	<15	I+ISII
AI-9	8.91	4.80	1.21	1.74	<15	I+ISII
AI-11	8.84	–	2.89	2.41	8	I+ISII
AI-19	8.81	–	2.44	2.23	<15	I+ISII
DI-3	8.78	5.10	2.06	2.24	6	I+ISII
HI-2	8.90	–	2.26	2.10	<15	I+ISII
HI-3	8.80	–	1.75	2.96	<15	I+ISII
HI-4	8.94	–	1.91	3.60	<15	I+ISII
HI-6	8.90	–	1.94	2.09	<15	I+ISII
HI-8	8.92	–	2.50	1.76	<15	I+ISII
HI-15	8.82	–	2.20	1.78	<15	I+ISII
HI-21	8.90	–	2.38	1.97	<15	I+ISII
HI-22	8.92	–	2.33	1.15	<15	I+ISII
TI-4	8.90	–	2.69	1.04	0	I
WI-7	8.83	–	2.54	2.12	<15	I+ISII
WI-10	8.83	–	2.71	2.17	<15	I+ISII
II-6	8.90	3.07	1.09	1.13	<15	I+ISII
CI-6	8.93	2.67	0.87	1.05	0	I
CI-11	8.92	5.15	2.61	1.04	0	I

[a] the angular distance between the 002 and 001 reflections from glycolated preparations.

[b] the joint breadth of 001 illite and adjacent illite/smectite reflections, measured in $^\circ 2\theta$ from where the tails of the X-ray background.

[c] the joint breadth of 004 illite and adjacent illite/smectite reflections, measured like BB1.

[d] the intensity ratios of the 001 and 003 reflections from the air-dried and glycolated samples.

1M and $2M_1$ polytypes, are detected in Sarisan mine (Fig. 5). Almost all samples are mixtures of 1M and $2M_1$ and pure 1M sample is rarely found.

Chemical analyses of illites (Table 2) show that charge deficiencies arise mainly from tetrahedral sheet and the interlayer cation is mostly K and rarely Na or Ca. Substitution of Al^{3+} for Si^{4+} are less than that of muscovite, giving the value of about 1/5-1/6. As a consequence of these smaller substitutions, the total layer charges are significantly less than 1 per $O_{10}(OH)_2$ giving the value of 0.768-0.926. These compositions are plotted on the illite field in compositional diagram of Velde (1985) (Fig. 6).

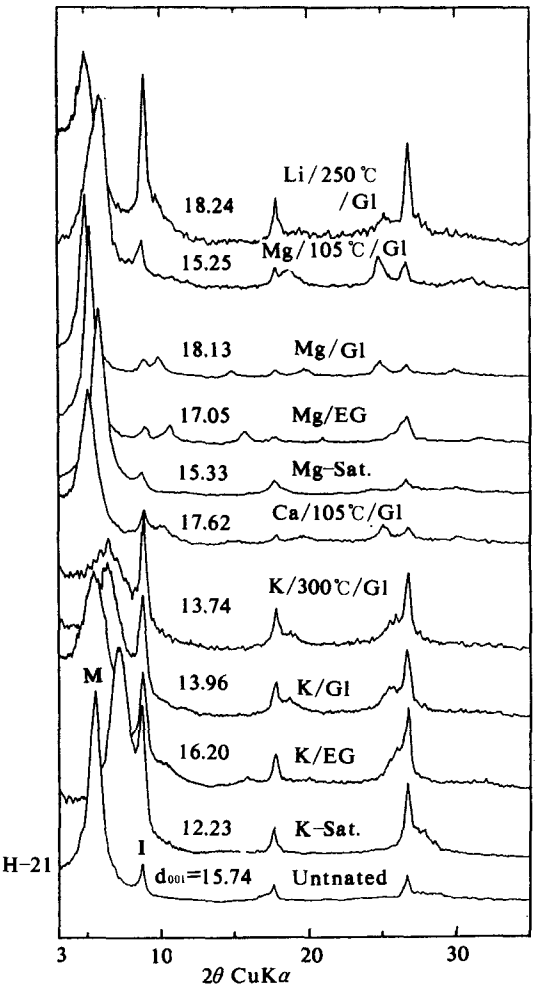

Fig. 8. X-ray diffraction patterns of montmorillonite treated with heat, various cations, and organic materials. M:montmorillonite, I:illite.

Scanning electron micrographs show that illite occurs as small, poorly defined flakes commonly grouped together in irregular aggregates (Fig. 7A, B). Occasionally some flakes show crude hexagonal outlines (Fig. 7B) or single euhedral outline (Fig. 7C).

Smectite

Smectites are closely associated with muscovite (Fig. 7). Most of smectites are found along the edges of muscovite grains. It suggests that smectite

has been formed by alteration of muscovite (Fig. 7D, E). They occur as irregular mossy, foliated or flake-shaped aggregates. Transmission electron micrograph (Fig. 7F) shows that the irregular fluffy aggregates of extremely small particles are admixed with discrete illite grains.

Smectites and interstratified clays containing smectitic component have been identified by XRD. The I/S interstratification was determined by Srodon's methods (1980) and the results are given in Table 3. Table 3 shows that the three methods give fairly similar results except for some by method II. According to Srodon (1980), the Δd_2 method is recommended as the most precise one. According to these determinations, most smectites from the Sarisan mine are not interstratified except for the rarely found random-interstratified I/S minerals with 80-98% smectite.

Smectite samples having the basal reflection in range from 14.4 to 15.7 Å were used for their detailed characterization by X-ray diffraction, various cation-saturation, solvation with organic materials, and heat treatment(Fig. 8).

Table 2. Electron microprobe analyses of illites from the Sarisan mine.

	H-22	H-12	H-13	D-9	I-6	H-23	G-12-2	G-3	G-21
SiO_2	47.76	45.64	48.95	47.48	48.39	47.13	47.03	48.71	48.32
Al_2O_3	33.30	30.20	32.11	31.86	33.66	34.66	32.75	33.76	32.42
TiO_2	0.10	0.01	0.04	0.05	0.15	0.08	0.16	0.24	0.15
Cr_2O_3	0.04	0.08	0.02	0.05	0.19	0.11	0.06	0.00	0.22
FeO*	2.16	4.47	2.49	2.72	1.30	1.81	2.11	1.90	2.38
MgO	0.86	1.08	1.00	1.01	1.17	0.40	0.61	1.12	0.93
MnO	0.15	0.09	0.00	0.04	0.01	0.00	0.00	0.13	0.01
CaO	0.02	0.07	0.04	0.13	0.03	0.08	0.04	0.03	0.03
K_2O	10.39	9.90	10.62	8.49	10.49	9.26	10.23	9.14	10.57
Na_2O	0.11	0.21	0.05	0.07	0.06	0.08	0.25	0.07	0.11
Total	94.85	91.74	95.31	91.88	95.45	93.60	93.24	95.10	95.14
	Numbers of cations on the basis of $O_{10}(OH)_2$								
Si	3.192	3.202	3.260	3.247	3.200	3.162	3.198	3.213	3.227
Al(IV)	0.808	0.798	0.740	0.753	0.800	0.838	0.802	0.787	0.773
SUM	4.000	4.000	4.000	4.000	4.000	4.000	4.000	4.000	4.000
Al(VI)	1.816	1.699	1.780	1.815	1.823	1.903	1.823	1.838	1.779
Ti	0.005	0.001	0.002	0.003	0.007	0.004	0.008	0.012	0.008
Cr	0.002	0.004	0.001	0.003	0.010	0.006	0.003	0.000	0.012
Fe	0.121	0.262	0.138	0.155	0.072	0.102	0.120	0.105	0.133
Mg	0.086	0.112	0.099	0.103	0.115	0.040	0.062	0.110	0.093
Mn	0.008	0.005	0.000	0.002	0.001	0.000	0.000	0.007	0.001
SUM	2.038	2.084	2.021	2.081	2.028	2.054	2.016	2.072	2.024
Ca	0.001	0.005	0.003	0.010	0.002	0.005	0.003	0.002	0.002
K	0.886	0.886	0.902	0.741	0.885	0.793	0.887	0.769	0.901
Na	0.014	0.029	0.006	0.009	0.008	0.010	0.033	0.009	0.014
SUM	0.902	0.920	0.911	0.759	0.895	0.808	0.923	0.780	0.917
Si/Al	1.216	1.282	1.293	1.264	1.220	1.154	1.218	1.224	1.265
Tet.	-0.808	-0.798	-0.740	-0.753	-0.800	-0.838	-0.802	-0.787	-0.773
Oct.	-0.095	-0.126	-0.173	-0.015	-0.096	0.024	-0.124	0.005	-0.146
Int.	0.903	0.924	0.914	0.768	0.897	0.814	0.926	0.782	0.919

* Total Fe as FeO

Table 3. Results of illite/smectite interstratification measurement by X-ray diffraction.

Sample No.	d(001) (EG, Å)	[a]Δd_2 (2θ)	%S from [b]method I	II	III
A-2	17.05		100	100	100
A-8	17.05	5.54	100	72	100
A-9	17.08	—	—	—	100
A-11	17.08	5.51	98	75	100
A-19	17.18	5.04	80	65	92
D-3	17.31	6.38	100	100	100
D-4	17.18	5.19	84	72	90
H-2	16.95	5.07	81	60	60
H-3	17.55	5.09	82	80	100
H-4	16.98	5.51	98	80	100
H-6	17.18	5.56	100	65	100
H-8	16.98	5.46	92	80	100
H-15	17.31	—	—	—	96
H-21	17.21	6.22	100	100	100
H-22	17.25	6.08	100	100	100
T-4	17.18	6.80	100	100	100
W-7	17.18	5.74	100	93	100
W-10	17.08	5.10	82	53	80

[a] the difference in 2θ of the two reflections on the region 42°-48° 2θ.

[b] Method I ; using the relation between Δd_2 and percent smectite layers. Method II ; using the stronger of the two reflections between 42°-48° 2θ and the strong reflection that migrates from about 26° to 27° 2θ. Method III ; using the peaks which migrate from about 26°-27° 2θ and from 15.4°-17.7° 2θ.

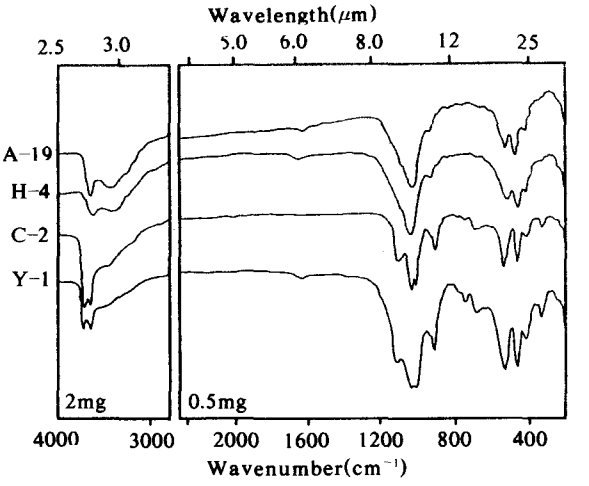

Fig. 9. Infrared absorption patterns of montmorillonite (A-19, H-4) and disordered kaolinite (C-2, Y-1) from the Sarisan mine.

19 different treatment for each of 18 smectite samples were systematically carried out according to the flow diagram by Thorez(1976) and some of the results are given in Table 4. The above experiment shows that most of smectites in Sarisan mine, excluding sample D-4 (beidellite), consist of montmorillonite. It shows 15.0-16.1 Å after Mg-saturation, 16.7-17.6 Å after Mg/EG, 16.1-

Table 4. d(001) values of various cation-saturated, organic solvated, and heat treated smectites from the Sarisan mine.

Sample No.	Untreated	EG	K	K/EG	K/Gl	K/300℃ /GL	Ca/105℃ /Gl	Mg	Mg/EG	MG/Gl	Li/250℃ /Gl
A-2	15.80	17.05	11.24	13.30	12.46	13.80	18.21	15.10	16.69	17.84	16.03
A-8	15.71	17.05	11.81	15.20	13.97	13.42	15.44	15.25	16.98	16.82	17.49
A-9	15.52	17.08	11.56	13.32	13.10	12.34	17.01	15.36	17.55	16.08	16.76
A-11	15.60	17.08	11.89	13.97	13.30	13.86	16.92	15.10	16.76	15.49	17.31
A-19	15.47	17.18	12.03	14.22	13.84	14.20	16.03	15.30	16.98	15.12	16.69
D-3	15.91	17.31	11.55	16.35	14.18	13.69	16.79	15.57	16.82	16.66	17.73
D-4	14.65	17.18	11.87	14.06	13.63	13.59	15.02	14.92	16.95	14.53	17.01
H-2	15.33	16.95	10.16	10.17	10.16	13.53	17.91	15.20	16.76	17.49	17.77
H-3	15.63	17.55	11.10	15.02	14.00	12.75	17.59	15.07	17.08	17.66	17.91
H-4	15.71	17.18	11.95	16.06	13.32	13.67	15.33	15.04	17.11	17.28	18.17
H-6	15.55	16.98	12.05	13.95	13.86	13.46	14.65	15.04	16.85	17.18	17.18
H-8	15.91	17.31	12.58	16.72	13.76	14.45	17.55	15.52	17.05	17.91	14.22
H-15	15.50	17.18	10.30	15.41	10.14	10.05	18.95	15.49	17.25	18.36	18.47
H-21	15.74	17.21	12.23	16.20	13.86	13.74	17.62	15.33	17.05	18.13	18.24
H-22	15.71	17.25	11.78	16.23	13.55	13.26	16.66	15.10	17.15	18.28	17.91
T-4	15.74	17.18	12.17	17.77	14.11	14.11	17.25	14.99	17.05	18.40	17.95
W-7	15.83	17.18	12.44	16.72	14.60	13.78	17.28	15.02	16.98	17.80	17.91
W-10	15.55	17.08	11.34	15.52	11.15	14.79	18.06	16.14	18.17	18.95	17.45

Table 5. pH values of smectites from the Sarisan mine.

Color	Sample No.	pH	Color	Sample No.	pH
Yellow	A-2	6.75	White	A-11	6.21
	A-8	6.03		W-7	7.40
	H-2	6.67	Pink	D-3	6.28
	H-4	6.13		H-21	6.52
Green	A-19	6.29	Brown	A-9	6.21
	H-3	7.02		D-4	5.54
	H-15	5.83		H-6	5.40
	W-10	6.45		H-8	5.47

18.4 Å after Mg/Gl, 16.0-18.2 Å after Ca/105°C/Gl, and 16.7-18.2 Å after Li/250℃/Gl. It also has high net layer charge judging from the data; 11.2-14.6 Å after K/Gl, 12.3-14.8 Å after K/300℃/Gl, and some questionably 10.3-12.6 Å after K-sat. and 13.3-17.8 Å after K/EG (Thorez, 1976).

pH values of clay suspensions were determined with a glass electrode. pH values range from 5.4 to 7.4 but most of them are neutral or weak acidic (Table 5). pH value is much related to cation exchange capacity and the origin and nature of the material (Bonneau and Souchier, 1982).

Infrared absorption spectra of montmorillonites from Sarisan mine are shown in Fig. 9. Characteristic absorption bands for montmorillonite in this study are at 3633-3620, 1124-1081, 1030-1023, 911, 875, 840-818, 796, 629-610, 522, 466 cm^{-1}, and they well coincide with van der Marel and Beutelspacher (1976), Farmer (1974), and Russell (1987).

With increasing substitution of Al^{3+} by Fe^{3+} in montmorillonite, the $AlFe^{3+}OH$ deformation band shifts from 890 to 870 cm^{-1} and, when sufficient iron is present to give $Fe^{3+}Fe^{3+}OH$ groupings as in nontronite, a band appears at 815 cm^{-1}. This low-frequency shift of OH stretching and deformation bands with increasing Fe^{3+} content is a very important criterion for the determination of ferruginous smectites in clay materials (Russell, 1987). The absorption patterns of montmorillonites in the study area show the $AlFe^{3+}OH$ deformation bands at 872-883 cm^{-1} region, and there is no 815 cm^{-1} band. Therefore, the montmorillonite in the study area is a Fe-rich one, not nontronite. This fact coincides with the above-mentioned thermal data.

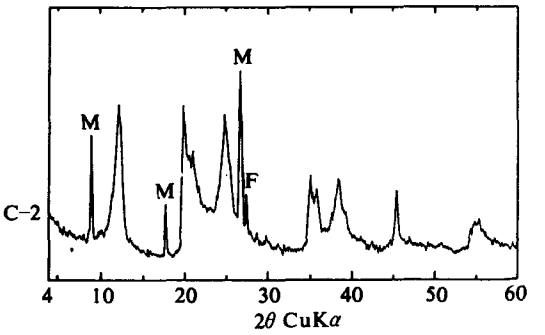

Fig. 10. X-ray diffraction pattern of disordered kaolinite from the Sarisan mine. M:mica, F:feldspar.

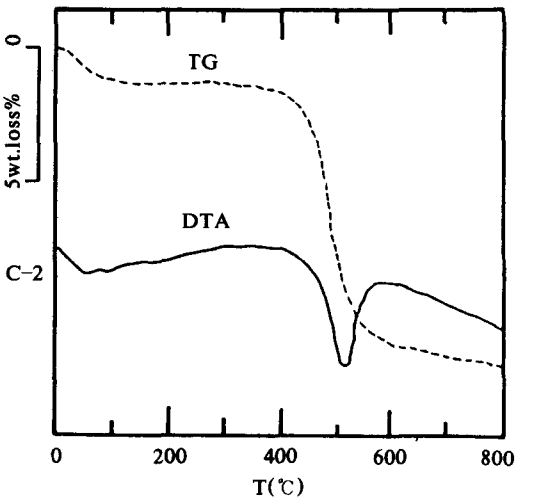

Fig. 11. DTA and TG curves of disordered kaolinite.

Disordered Kaolinite

X-ray diffraction study shows that the kaolinite from the study area is of disordered type (Fig. 10). The 001 peak (7.21 Å) is not sharp and intense as compared with well-crystallized kaolinite, suggesting some occasional interlayer water between the kaolinite units. Thermal data also suggest the presence of such water. Disordered kaolinite is characterized by the considerably blurred peak between 20° and 30° 2θ and doublets for (131) and (201) peaks in the range from 35° -40° 2θ (Figure. 10).

DTA and TG curves of the disordered kaolinite are shown in Figure. 11. The low-temperature endothermic peak at around 100℃ is due to the loss of adsorbed water. This fact indicates that, if there is irregularity in the arrangement of the kaolinite units, a small amount of water may be present between the layers. This is in accordance with the slightly larger c-spacing of the disordered kaolinite. In general, the removal of the hydroxyls takes place from 450℃ to 600℃. The endothermic peak temperature of the disordered kaolinite in the present study is 511℃ (Fig. 11). This deviation can be explained by variations in particle size, since the dehydration temperature is known to decrease with decreasing particle size. But, this deviation may also be due to the crystallinity than to the particle size, since the poorly crystalline kaolinite loses its hydroxyl water somewhat more readily than the well-crystallized one (Grim, 1968; Todor, 1976).

Chemical analyses (Table 6) show that the Al/Si ratios of the disordered kaolinites differ from unity by only a few percent. There is only a slight substitution of iron for aluminum in kaolinite. Such substitutions are restricted to the poorly crystallized kaolinite (Grim, 1968). The kaolinite contains 0.1% Cr_2O_3. According to Maksimovic et al. (1981), chromium replaces aluminum in octahedral sites. This substitution is facilitated by the similarity in ionic size (Cr_{VI}^{3+}=0.70 Å, Al_{VI}^{3+}=0.61 Å) (Whittaker and Muntus, 1970).

Infrared absorption spectrum of the disordered kaolinite from Yeoju area shows bands at 3703, 3629 cm^{-1} doublet which are characteristic for the kaolin group (Fig. 9). Disorder in kaolinite is detectable mainly in the OH-stretching region, although some general broadening of all bands in the spectrum may also occur (Russell, 1987). The 3669, 3652 cm^{-1} doublet for the well-crystallized kaolinite is replaced by a single broad band at 3653 cm^{-1}. Two weak bands are also found at 788 and 747 cm^{-1} as for the well-crystallized kaolinite, but the 788 cm^{-1} band is reduced to a very weak one.

Scanning electron micrograph (Fig. 7G) shows some book structure of kaolinite and etch pits in plagioclase. Kaolinite is the alteration product of plagioclase.

Table 6. Electron microprobe analyses of disordered kaolinites from the Sarisan mine.

	A108	A110	A115	A116
SiO_2	44.52	44.00	45.53	46.86
Al_2O_3	39.85	39.33	39.44	40.56
TiO_2	0.00	0.00	0.00	0.00
Cr_2O_3	0.12	0.11	0.08	0.12
Fe_2O_3*	0.49	0.24	0.00	0.36
MgO	0.07	0.00	0.10	0.00
MnO	0.00	0.00	0.19	0.00
CaO	0.15	0.08	0.14	0.11
K_2O	0.12	0.10	0.00	0.00
Na_2O	0.04	0.08	0.04	0.00
Total	85.36	83.94	85.52	88.01
Numbers of cations on basis of $O_{10}(OH)_8$				
Si	3.885	3.897	3.950	3.952
Al(IV)	0.115	0.103	0.050	0.048
SUM	4.000	4.000	4.000	4.000
Al(VI)	3.984	4.002	3.982	3.984
Ti	0.000	0.000	0.000	0.000
Cr	0.008	0.008	0.005	0.008
Fe	0.036	0.018	0.000	0.025
Mg	0.009	0.000	0.013	0.000
Mn	0.000	0.000	0.014	0.000
SUM	4.037	4.027	4.015	4.018
Ca	0.014	0.008	0.013	0.010
K	0.013	0.011	0.000	0.000
Na	0.007	0.014	0.007	0.000
SUM	0.034	0.033	0.020	0.010
Al/Si	1.055	1.053	1.021	1.020

* Total Fe as Fe_2O_3

Vermiculite

In Yeoju area, vermiculite occurs as macroscopic particles in association with biotite. Scanning electron micrograph (Fig. 7H) shows that biotite transformed into vermiculite. The alteration of biotite to vermiculite implies the replacement of the interlayer potassium by hydrated cation, generally magnesium.

In order to identify vermiculites, X-ray dif-

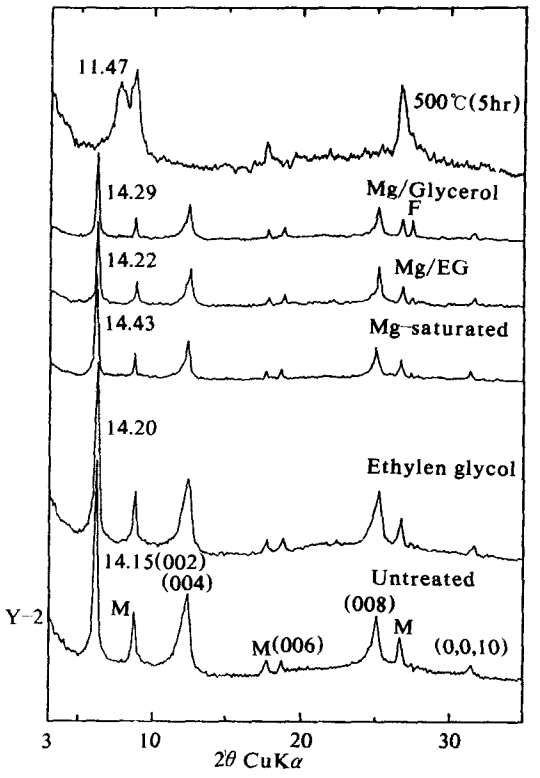

Fig. 12. X-ray diffraction patterns of vermiculite treated with heat, organic materials, and various cations. M:mica, F:feldspar.

fraction analysis was performed on Mg-saturated, organic material-solvated and heat-treated samples. The results are shown in Fig. 12. They indicate that vermiculite from the study area is a high-charged trioctahedral one. It can be distinguished from chlorite by the relative intensity of the (001) reflection (Thorez, 1976).

DISCUSSION ON CLAY MINERAL FORMATION

The genetic study of the alteration products is complicated by the difficulty of distinguishing hypogene minerals from supergene ones, especially in clay deposits which have been subjected to the low temperature hydro thermal alteration. The low temperature hydrothermal alteration is similar to the weathering alteration in which the physical arrangements and chemical potentials are guided by the same factors (Velde, 1985). If alkalies and alkaline earth elements, except potassium, are present, the micas and the plagioclase feldspars are likely to yield smectite. The presence of magnesium particularly favors the formation of smectite. The presence of potash, either from feldspars or primary micas, favors the development of illites (Grim, 1968). Therefore, illite is presumably formed in hydrothermal environments where the solution have a high K/H ratio. The low K/Na and K/Mg ratios favor the formation of smectite minerals. Another important factor for mineral formation is the changes in environmental conditions.

The mineral association in the Sarisan clay deposits suggests that the hydrothermal alteration is superimposed by later weathering alteration. Illite and smectite were formed by hydrothermal alteration of two-mica granite. Smecite was formed only in the vein clay along the quartz vein, where illite is found as wide zone in both side of quartz vein and also in vein clay. The distribution pattern of illite and smectite suggests that both mineral have been formed by hydrothermal alteration of two-mica granite.

Illite was formed by the destruction of the K-feldspars. The highly illitic interstratified minerals were formed from illite during later weathering. According to Yoder and Eugster (1955) and Velde (1965), the sequence 1Md-1M-$2M_1$ is found with increasing hydrother-mal run time and temperature. Illites from the study area are of 1M and $2M_1$ types.

It is also observed under the microscope that feldspar in the two-mica granite in both side of quartz vein is altered to smectite. High grade clay is found along the wall of the quartz vein forming the ridge of Mt. Sari (Fig. 3C). It can be considered that sericite (illite) and smectite were formed from feldspar during the hydrothermal alteration by the hydro-thermal solution which formed the

quartz vein. The homogenization temperature of fluid inclusions in quartz from Sarisan quartz vein were measured to be 200℃ to 275℃. Disordered kaolinite and vermiculite were for med from plagioclase and biotite, respec tively, by the weathering process.

CONCLUSIONS

Clay from the Sarisan mine consists mainly of montmorillonite, discrete illite, and highly illitic interstratified minerals. In some samples, it includes the randomly interstratified I/S which is in the compositional range of 80–98% smectite.

Weathering alteration is less important than hydrothermal alteration for the formation of illite and smectite minerals. It appears that illites were formed in the early stage and smectite in the late stage. Smectite clay consists of montmorillonite with high negative charge. Illite has a low lattice charge (0.768–0.926 per $O_{10}(OH)_2$), low K^+ content (0.741–0.902 per $O_{10}(OH)_2$), and high Si/Al ratio (1.154–1.293) relative to muscovites. They consist of 1M and $2M_1$ polytypes. Homogenization temperatures of fluid inclusions from quartz veins, which probably affected the formation of the clay minerals directly or indirectly, range from 200℃ to 275℃.

Other clay minerals such as disordered kaolinite and vermiculite, are weathering products of plagioclase and biotite, respec tively, in the supergene environment.

REFERENCES

Bailey, S.W. (1980) Summary of recommendations of the AIPEA Nomenclature Committee. Can. Miner., 18, 143–150.

Bonneau, M. and Souchieer, B. (1982) Constituent and Properties of Soils. Academic Press. 43–81.

Brewster, G. R. (1980) Effect of chemical pretreatment on X-ray powder diffraction characteristics of clay minerals derived from volcanic ash. Clays Clay Miner., 28, 303–310.

Brindley, G. W. and Brown, G. (1980) Crystal Structures of Clay Minerals and Their X-ray Identification: Mineralogical Society Monograph No. 5. Min. Soc., London.

Farmer, V. C. (1974) The Infrared Spectra of Minerals. Min. Soc., London, 331–363.

Gaudette, H. E., Eades, J. L. and Grim, R. E. (1966) The nature of illite. Clays Clay Miner. Proc., 13, 33–48.

Grim, R. E. (1968) Clay Mineralogy. 2nd ed. McGraw-Hill.

Jackson, M. L. (1969) Soil Chemical Analysis-Advanced course. 2nd ed. University of Wisconsin, Madison, WI.

Korea Mining Promotion Corporation (1980) Report on the Properties of Non-Metallic Minerals (in Korean).

Maksimovic, Z., White, J. L. and Logar, M. (1981) Chromium-bearing dickite and chromium-bearing kaolinite from Teslic, Yugoslavia. Clays Clay Miner., 29, 213–218.

Russell, J. D. (1987) Infrared methods. In: Wilson, M. J. A Handbook of Determinative Methods in Clay Mineralogy. Blacki, 133–173.

Srodon, J. (1980) Precise identification of illite/smectite interstratifications by X-ray powder diffraction. Clays Clay Miner., 28, 401–411.

Srodon, J. (1984) X-ray powder diffraction identification of illitic materials. Clays Clay Miner., 32, 337–349.

Srodon, J. and Eberl, D. D. (1984) Illite. In: Bailey, S. W. Micas. Reviews in Mineralogy. 13, Min. Soc. Amer. 495–544.

Thorez, J. (1976) Practical Identification of Clay Minerals. Institute of Mineralogy, Liege State Univ., Belgium, 8–36.

Todor, D. N. (1976) Thermal Analysis of Minerals. Abacus Press. 210–243.

van der Marel, H. and Beutelspacher, H. (1976) Atlas of Infrared Spectroscopy of Clay Minerals and Their Admixtures. Elsevier, Amsterdam.

Velde, B. (1965) Experimental determination of

muscovite polymorphs stabilities. Amer. Miner., 50, 436-449.

Velde, B. (1985) Clay minerals: A Physico-Chemical Explanation of Their Occurrence. Elsevier Scientific Publishing Company, 38-169.

Whittaker, E. J. W. and Muntus, R. (1970) Ionic radii for use in geochemistry. Geochim. Cosmochim, Acta, 8, 225-280.

Yeo, S. C. and Lee, I. K. (1975) Geological Map of Yeoju Sheet, Scale 1:50,000. Geological and Mineral Institute of Korea (in Korean).

Yoder, H. S. and Eugster, H. P. (1955) Synthetic and natural muscovites. Geochem. Cosmochim, Acta, 8, 225-280.